2D Magnetic Design and Optimization of a 88-mm Aperture 15 T Dipole for NED

Nikolai Schwerg, Christine Vollinger, Arnaud Devred and Daniel Leroy

***Abstract*—The Next European Dipole (NED) activity supported by the European Union aims at the development of a high-performance Nb_3Sn conductor (J_c=1500 A/mm^2 @ 15 T, 4.2 K) in collaboration with European industry and at the design of a high-field dipole magnet making use of this conductor. In the framework of the NED collaboration which coordinates the activity of several institutes, CERN has contributed to the electromagnetic design study of a cos-θ, layer-type superconducting dipole with an 88 mm aperture that is able to reach 15 T at 4.2 K. Part of the optimization process was dedicated to the reduction of the multipole coefficients so as to improve field quality while keeping an efficient peak-field to main-field ratio. In this paper, we present the optimization of the coil cross-section and of the shape of the iron yoke to reduce saturation-induced field errors during ramp. The effects of persistent magnetization currents are also estimated and different methods to compensate persistent-current-induced field distortions are presented.**

***Index Terms*— high field dipole magnet, iron yoke saturation, Nb_3Sn, persistent magnetization currents**

I. Introduction

In the framework of the EU-funded Coordinated Accelerator Research in Europe (CARE) project, the Next European Dipole (NED) activity is dedicated to the development of a high-field dipole magnet using Nb_3Sn conductors [1]. Part of the NED activity, which is shared amongst several collaborating institutes, is a design study of different possible dipole configurations able to reach 15 T at quench [2].

In this paper, the results of the electromagnetic design study for the cos-θ, layer-type dipole are presented [3]. The studied dipole is an 88-mm large-bore, single-aperture dipole surrounded by an iron yoke. It relies on specifications for the Nb_3Sn strand and the Rutherford-type cable, as well as on material properties, salient dimensions and maximum allowable stress agreed upon by the NED collaboration [1]- [4].

All calculations are carried out by means of the CERN field computation program ROXIE [5] using the intersecting-ellipse model for the simulation of persistent-current-induced field errors [6]. The field quality in the aperture is described in terms of normalized harmonic coefficients according to:

$$B_y(x,y) + iB_x(x,y) = 10^{-4} \times B_{\mathrm{ref}} \sum_{n=1}^{\infty} (b_n + ia_n) \left(\frac{x+iy}{r_0} \right)^{n-1}$$

where $B_x(x,y)$ and $B_y(x,y)$ are the horizontal and vertical field components, B_{ref} the main field component at the reference radius r_0 and b_n and a_n the normal and skew harmonic coefficients.

Starting from the results of the preliminary design study presented in [4], the coil cross-section was optimized with respect to field quality and conductor alignment. The iron yoke was shaped in order to minimize the influence of the iron saturation on the relative multipole field errors during ramp. In addition, a study of different methods for the compensation of persistent-current-induced field errors was carried out.

II. Geometry

A. Coil Cross-Section

The cable specifications for the cos-θ, layer-type NED design are: a keystone angle of 0.44°, a width of 26 mm and an average thickness of 2.275 mm. The cable width is of the same order of magnitude as the aperture diameter of 88 mm. Hence, the electromagnetic design for NED has to satisfy stringent requirements on conductor placement. In order to facilitate the winding and improve the conductor support, we aimed to put the conductors in a radial position. For this purpose, the abso-

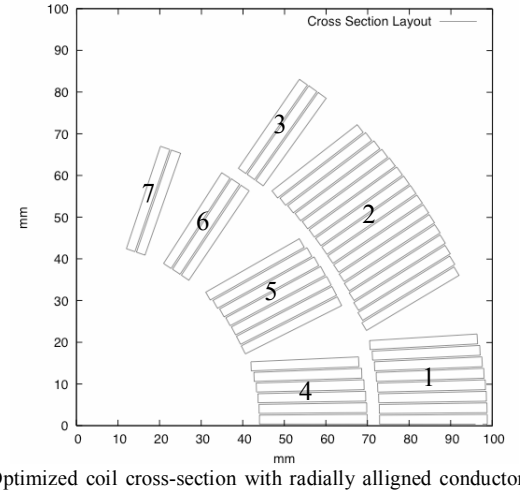

Fig. 1. Optimized coil cross-section with radially alligned conductors (after re-optimization including the elliptical iron yoke). The numbers represent the block numbers.

Manuscript received August 29, 2006. This work was supported in part by the European Community–Research Infrastructure Activity under the FP6 "Structuring the European Research Area" program (CARE, contract number RII3-CT-2003-506395).

N. Schwerg, D. Leroy, and C. Vollinger are with CERN AT/MAS, CH-1211 Geneva 23, Switzerland (Corresponding author is N. Schwerg, email: Nikolai.Schwerg@cern.ch, phone: +41-227679583).

A. Devred is with CEA/Saclay DSM/DAPNIA/SACM, 91191 Gif-sur-Yvette, CEDEX, France, and CERN AT/MAS.

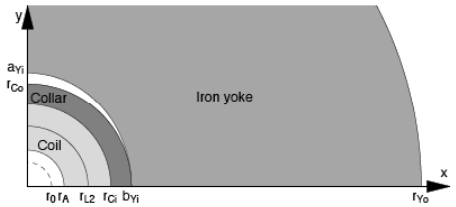

Fig. 2. Cross-section of the optimized elliptical iron yoke.

lute value of the difference between the mean inclination angle and the mean positioning angle is summed block-wise and used as objective for the optimization. Consequently, in the resulting cross-section as shown in Fig. 1, all conductor blocks are radially aligned, with the exception of block 5.

B. Iron Yoke

We observed strong iron saturation effects with varying energization currents due to the high magnetic field and the proximity of the iron yoke. A partial compensation could be reached with an iron yoke with elliptical inner contour, that gives a reduction of the amount of iron material in the area where saturation starts first [7]. This allows a steering of the field variation during ramp up, especially for b_3 and b_5, with only small losses in main field strength. The iron geometry is illustrated in Fig. 2 whereas Table I shows salient parameters.

The electromagnetic properties of the optimized cross-section at high field (8.5% margin on the load line) and at quench field are shown in Table II.

The relative multipole errors at high field are presented in Table III. These exhibit extremely small values for all multipoles except b_9 and b_{11} which are acceptable but stayed in the order of 1 to 3 units and could not be further reduced by design. Figure 3 shows the variation of the multipole errors versus energization current for both the circular iron yoke with an inner radius of 125.4 mm and for the elliptical yoke. (Superconductor magnetization effects are not considered.) The total variation of b_3 was reduced from 16.1 to 5.4 units and the variation of b_5 from 0.59 to 0.51 units. The elliptical yoke is used as final design.

TABLE I SALIENT PARAMETER OF NED MAGNET CROSS-SECTION

Quantity	Value	Unit
Reference radius r_0 for field errors	29	mm
Aperture radius r_A	44	mm
Inner yoke semi minor axis b_{yi}	125.4	mm
Inner yoke semi major axis a_{yi}	138.6	mm
Outer yoke radius r_{Yo}	475.4	mm

TABLE II SALIENT ELECTROMAGNETIC PROPERTIES AT HIGH FIELD (8.5% MARGIN ON THE LOAD LINE)

Quantity	Value	Unit
Maximum energization current	26670	A
Main field B_1	13.31	T
Peak field on conductor B_{peak}	13.75	T
Peak field / main field	1.032	-
Energization current at quench	29440	A
Peak field at quench	15.00	T

TABLE III RELATIVE MULTIPOLE FIELD ERRORS (UNITS @ 29 MM) AT HIGH FIELD (8.5% MARGIN ON THE LOAD LINE)

b_3	b_5	b_7	b_9	b_{11}	b_{13}	b_{15}
-0.02	0.06	0.08	1.70	2.69	-0.05	-0.18

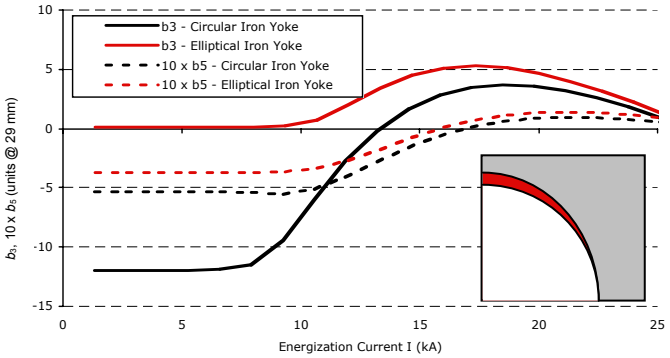

Fig. 3. Multipole variation due to iron saturation for the initial circular and the final elliptical iron yoke.

III. PERSISTENT-CURRENT-INDUCED FIELD ERRORS

The calculation of the persistent-current-induced field errors relies on an estimation of the critical current density of the NED strand. However, measurement data became available only very recently [8]. Therefore, we took the measurement data of a similar strand [9] that was scaled and fitted according to the NED cable specifications as shown in Fig. 4 [10].

All geometry intrinsic multipole field errors show a large variation and a hysteresis, especially for the low order ones such as b_3 and b_5. The variation of the multipoles b_3 to b_9 versus energization current are shown in Fig. 5.

The major goal was reducing the variation of the lower-order multipole field errors during ramp in a way that would cause only a small reduction of the main field and little detoriation on the higher order multipole field errors.

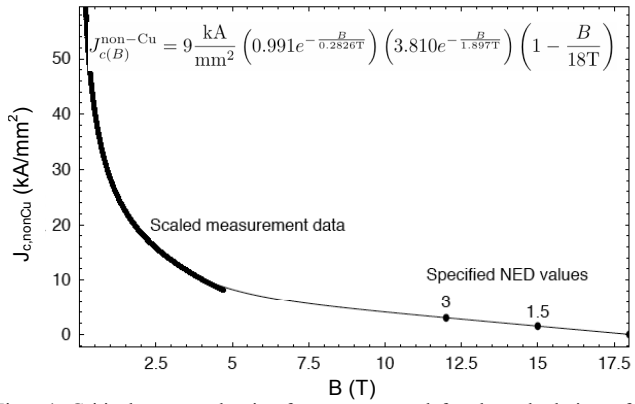

Fig. 4. Critical current density function as used for the calculation of the persistent-current-induced field errors.

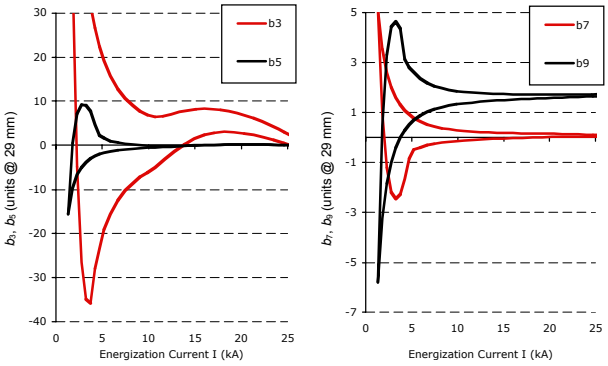

Fig. 5. Persistent-current-induced field errors without any compensation.

A. Passive Compensation Methods

Ferromagnetic materials exhibit a magnetization behavior of opposite sign compared to that of superconductors. When the material starts to saturate its relative contribution decreases. By adding ferromagnetic elements to the cross-section, the field error at low energization can be compensated without influencing the field quality at higher levels. This concept was proposed in [11] and studied in detail by others also (*e.g.* [12]). Therefore, the field errors that stem from the coil cross-section layout, the iron yoke and the additional ferromagnetic elements are designed such that they present the inverse behavior of the persistent-current-induced field errors on the up ramp.

The most efficient positions for these ferromagnetic elements can be found by simulating the influence of a thin permeable rod. The magnetic momentum per unit length, $\mathbf{m}'_{\mathrm{rod}}$, of a thin rod in an average local field, $\mathbf{B}_{\mathrm{loc}}$, is given by

$$\mathbf{m}'_{\mathrm{rod}} = \pi r_{\mathrm{rod}}^2 \frac{\mu_{\mathrm{rod}}/\mu_0 - 1}{\mu_{\mathrm{rod}}} \mathbf{B}_{\mathrm{loc}} \tag{1}$$

where μ_{rod} denotes the permeability and r_{rod} the radius of the rod. Taking into account the same symmetries as for the magnet itself, only odd normal multipoles are induced. The resulting multipole field components are [6]

$$\Delta B_n = \frac{\mu_0}{2\pi} \frac{r_0^{n-1}}{\rho_0^{n+1}} n \left[m_{\rho_0} \sin(n\phi_0) - m_{\phi_0} \cos(n\phi_0) \right] \tag{2}$$

where r_0 denotes the reference radius, (ρ_0, ϕ_0) the position of the rod and $m_{\rho 0}$ as well as $m_{\phi 0}$ denote the components of the magnetic momentum in the local orthonormal coordinate system (ρ_0, ϕ_0, z). Equation (2) enables the computation of the influence of a thin ferromagnetic rod based on the magnetic field inside the magnet's cross-section.

In Fig. 6, this is demonstrated for the presented coil cross-section but with a circular iron yoke. The white areas indicate positions of positive contribution, *i.e.* where the ΔB_n normalized to the overall maximum is positive, and the black areas show negative contribution. Since b_3 and b_5 have to be influenced in opposite directions, *i.e.* b_3 lifted up whereas b_5 reduced the sector between around 45° to 60° seems to be very promising.

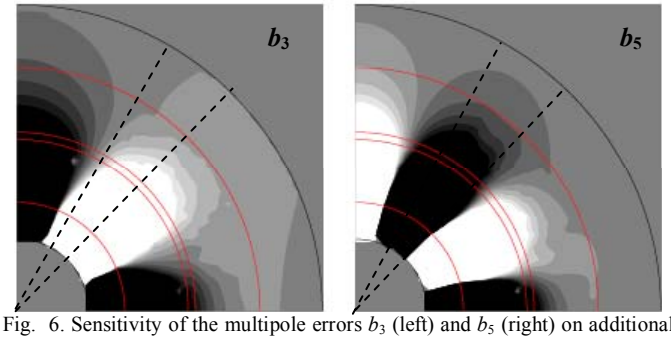

Fig. 6. Sensitivity of the multipole errors b_3 (left) and b_5 (right) on additional ferromagnetic elements.

1) Ferromagnetic Shims Inside the Cable

Similar to [13] a ferromagnetic shim of 20 mm width and 0.1 mm thickness is inserted between the two strand layers of the Rutherford-type cables. Since the same cable is used for the inner and outer layer of the NED magnet, the only free parameter is the shim thickness.

As shown in Fig. 7, the relative multipole error b_3 is lifted up by approximately 40 units and well compensates the original variation. The effect on b_5 is much less pronounced and in addition goes in the wrong direction (detoriation). The effect on b_7 and b_9 is very small.

The effect of ferromagnetic shims inside the cable was studied for the LHC main bending magnets in [14], but there it was found to be too strong. It was further assumed that for a cable with thicker strands and thus higher magnetization the method would work better what is well supported by our results. Nevertheless, the method of ferromagnetic compensation shims inside the cables is not considered, because it shows only limited steering possibilities, the permeable material is stress sensitive and the deformation of the shims during cabling, winding and operation is unknown.

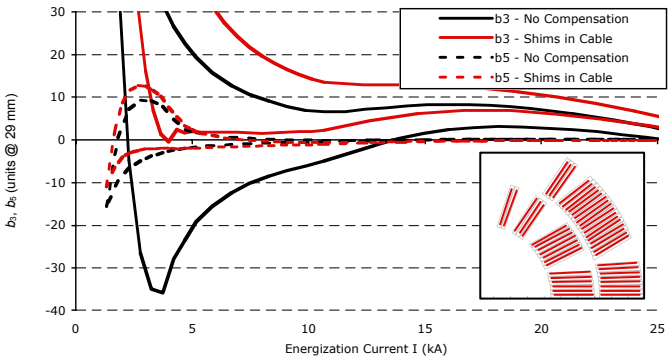

Fig. 7. Compensation of persistent-current-induced field errors by means of ferromagnetic shims inside the cable.

2) Ferromagnetic Shims on the Cold Bore Tube

A ferromagnetic sector is placed on the so-called cold bore tube (CBT) whose outer radius is assumed to be of 42 mm. Here, the optimization process has 3 free parameters: the angular position, the angular extension and the thickness. In good agreement with the analytical estimations, the best results are obtained for a shim of 0.507 mm thickness extending between 41.73° and 60.96°.

This method works well for the compensation of b_3, but b_5 is only partially compensated for values above 3 kA (Fig. 8).

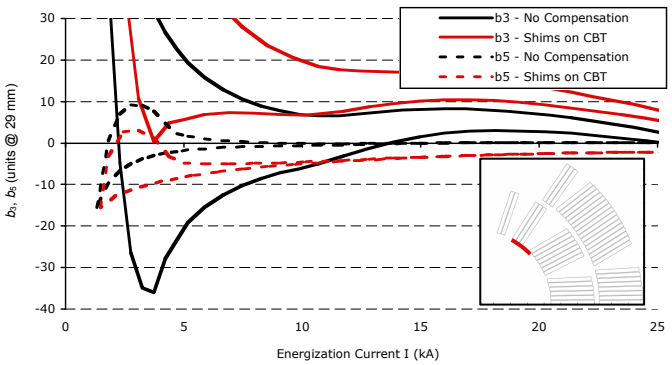

Fig. 8. Compensation of persistent-current-induced field errors by means of a ferromagnetic sector placed on the cold bore tube.

By increasing the distance of the ferromagnetic sector to the magnet center, the influence on the higher order multipole errors could be decreased. Therefore simulations with a ferromagnetic sector on the coil protection sheet between coil and collar were carried out but showed only a very small overall effect (only 10%).

3) Ferromagnetic Shims on Wedges

In the preliminary design study, the compensation of persistent-current-induced field errors was studied by means of ferromagnetic wedges replacing the non-magnetic copper wedges [4]. The study showed a very strong effect on b_3, much larger than necessary for the compensation. By reducing the size of the ferromagnetic part of the wedge, the saturation starts earlier and the overall effect can be reduced. For the design presented here, this is done by shims on one of the broad surfaces of the wedge. The presented compensation relies on two 26-mm-wide shims with different thicknesses, one placed in the inner layer and the other in the outer layer (as shown in Fig. 9). The inner layer shim is situated on top of block 5 and is 0.7 mm thick whereas the shim in the outer layer is on top of block 2 and is 1.5 mm thick.

The simulated multipole errors for the compensation with the two specified shims are shown in Fig. 9. It can be seen that the variation of b_3 is strongly reduced. Also, the variation of b_5 is decreased and even slightly over compensated. The variations of b_7 and b_9 have been amplified [3].

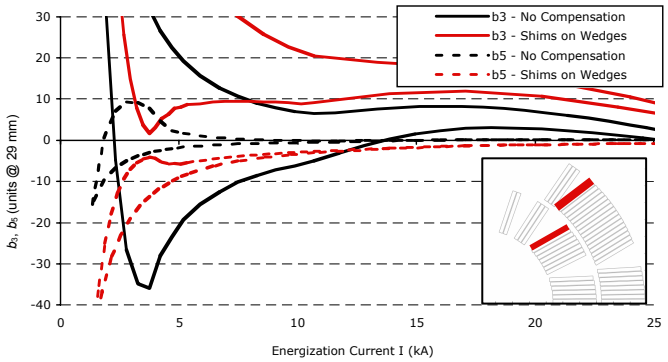

Fig. 9. Compensation of persistent-current-induced field errors by means of shims on wedges.

B. Active Compensation Method

Since the superconductor magnetization is the strongest in regions of the coil cross-section with low values of magnetic induction, the overall effect can be reduced if the field is locally enhanced by additional conductors or by conductors powered independently. Although this solution is not practical, Figure 10 presents as an exercise preliminary results obtained in the case where the outer layer mid plane conductor is independently powered at a higher current. While the energization current is ramped from 0 to 10 kA, in the midplane conductor an additional current is down ramped from 3 kA to 0. From simulation results, this method shows a remarkable reduction of the hysteresis width in b_3.

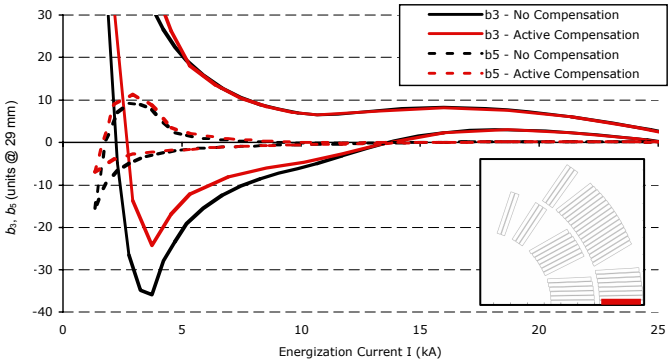

Fig. 10. Compensation of persistent-current-induced field errors by means of active elements. Here the individual powering of the first conductor.

IV. Conclusion

The cos-θ, layer-type dipole for NED has been re-optimized to improve geometric multipole coefficients. Its conductor blocks assume close to radial positions and its elliptical yoke enables a significant reduction of the saturation effects. The expected persistent-current-induced field errors of the NED cable have been simulated and it has been shown that the superconductor magnetization effects can be reduced by additional ferromagnetic shims on the wedges. The design is now used as reference design 2 for NED.

References

[1] A. Devred, *et al.*, "Overview and status of the Next European Dipole (NED) joint research activity," Supercon. Sci. Technol., vol. 19, pp. 67–83, Mar. 2006.

[2] F. Toral, *et al.*, "Comparison of 2-D magnetic and mechanical designs of selected coil configurations for the Next European Dipole," *IEEE Trans. Appl. Supercond.*, submitted for publication.

[3] N. Schwerg, "Electromagnetic design study for a large bore 15 T superconducting dipole magnet," diploma thesis, Technische Universität Berlin, Berlin, Germany, EDMS no. 722252, Nov. 2005.

[4] D. Leroy, "Cable design and R&D for NED," in Workshop on Accelerator Magnet Superconductors 2004, Archamps, France, Mar. 2004.

[5] S. Russenschuck, Electromagnetic design and optimization of accelerator magnets, 2nd ed. Geneva, Switzerland, ISBN: 92-9083-242-8, 2005.

[6] C. Vollinger, "Superconductor magnetization modeling for the numerical calculation of field errors in accelerator magnets," Ph.D. dissertation, Technische Universität Berlin, Berlin, Germany, Oct. 2002.

[7] G. Morgan, "Use of an elliptical aperture to control saturation in closely-coupled, cold iron, superconducting dipole magnets." *IEEE Trans. Nucl. Sci.*, vol. NS-32, pp. 3695–3697, Oct. 1985.

[8] P. Fabbricatore, *et al.*,"Investigation of magnetization behavior of Nb_3Sn wires for the Next European Dipole (NED) activity", *IEEE Trans. Appl. Supercond.*, submitted for publication.

[9] A. den Ouden, *et. al.*, "Progress in the development of an 88-mm bore 10 T Nb_3Sn dipole magnet," in *IEEE Trans. Appl. Supercond.,* vol. 11, pp. 2268–2271, Mar. 2001.

[10] N. Schwerg and C. Vollinger, "Development of a current fit function for NbTi to be used for calculation of persistent-current-induced field errors in the LHC main dipoles," in *IEEE Trans. Appl. Supercond.*, vol. 16, pp. 1828–1831, June 2006.

[11] M. A. Green, "Control of the fields due to superconductor magnetization in SSC magnets," in *IEEE Trans. Magn.*, MAG-23(2), pp. 506-9, 1987.

[12] V. V. Kashikhin, *et al.,* "Passive correction of the persistent current effect in Nb_3Sn accelerator magnets," in *IEEE Trans. Appl. Supercond.,* vol. 13, pp. 1270-1273, June 2003.

[13] V. V. Kashikhin and A. V. Zlobin, "Correction of the persistent current effect in Nb_3Sn dipole magnets," in *IEEE Trans. Appl. Supercond.,* vol. 11, pp. 2058-2061, Mar. 2001.

[14] C. Vollinger, M. Aleksa and S. Russenschuck, "Compensation of magnetization effects in superconducting accelerator magnets," *IEEE Trans. Appl. Supercond.*, vol. 12, no.1 pp. 1492- 1495, Mar. 2002.